NÖHÜ Müh. Bilim. Derg. / NOHU J. Eng. Sci., 2023; 12(4), 1615-1620

Niğde Ömer Halisdemir Üniversitesi Mühendislik Bilimleri Dergisi
Niğde Ömer Halisdemir University Journal of Engineering Sciences

Araştırma makalesi / Research article

www.dergipark.org.tr/tr/pub/ngumuh / www.dergipark.org.tr/en/pub/ngumuh

Friction stir spot weld (FSSW) of AZ91 magnesium alloys; effect of axial force and rotational speed on weld quality and an approach on inspection planning

AZ91 magnezyum alaşımlarının sürtünme karıştırma nokta kaynağı; eksenel kuvvet ve dönme hızının kaynak kalitesine etkisi ve muayene planlamasına ilişkin bir yaklaşım

Yasin Sarıkavak[1,*]

[1] *Ankara Yıldırım Beyazıt University, Department of Mechanical Engineering, 06010, Ankara, Türkiye*

Abstract

In this study, the friction stir spot welding (FSSW) process for the magnesium alloy (AZ91) sheet materials are investigated. Friction stir spot welding (FSSW) is a solid-state welding process and one of the innovative methods to join specifically automotive components. Recently magnesium alloys are promising materials where combination of high strength and low density can be observed to improve vehicle performance and reduce emissions and fuel consumption in structural materials for automotive applications. A finite element model (FEM) established to understand the effect of axial force and rotational speed during the simulation in automotive applications. The FEM investigates the effect of axial force ranging from 1 kN to 8 kN and rotational speeds of 1000 rpm - 4000 rpm. The model analyses the heat flux and the temperature rise that leads defect formation after the process. 4.5 kN, 6 kN and 8 kN axial forces and 3000 rpm-4000 rpm rotational speeds are evaluated as the critical values in terms of defect and crack formation during the process under specified boundary conditions. Finally, several non-destructive inspection methods are suggested to secure structural integrity after the FSSW process to eliminate the harmful effects of surface and volumetric discontinuities.

Keywords: Friction stir spot weld (FSSW), Finite element analysis (FEM), Magnesium alloy (AZ91), Axial force, Rotational speed, Nondestructive testing

Öz

Bu çalışmada magnezyum alaşımlı (AZ91) sac malzemeler için sürtünme karıştırma nokta kaynağı işlemi incelenmiştir. Sürtünme karıştırma nokta kaynağı, katı hal kaynak işlemidir ve özellikle otomotiv bileşenlerini birleştirmek için kullanılan yenilikçi kaynak yöntemlerinden biridir. Son yıllarda magnezyum alaşımları, otomotiv uygulamalarına yönelik yapısal malzemelerde araç performansını artırmak ve emisyonları ve yakıt tüketimini azaltmak için yüksek mukavemet ve düşük yoğunluk kombinasyonunun gözlenebildiği umut verici malzemelerdir. Otomotiv uygulamalarında eksenel kuvvet ve dönme hızının malzeme üzerine etkisini anlamak için bir sonlu elemanlar modelleştirilmiştir. Sonlu elemanlar modeli ile 1 kN ile 8 kN arasında değişen eksenel kuvvetin ve 1000 rpm - 4000 rpm arasındaki dönme hızlarının etkisini araştırılmıştır. Model, işlem sonrasında süreksizlik oluşumuna yol açan ısı akışını ve sıcaklık artışını analiz etmektedir. 4,5 kN, 6 kN ve 8 kN eksenel kuvvetler ve 3000 rpm-4000 rpm dönme hızları, belirlenen sınır şartları altında süreksizlik oluşumu açısından kritik işleme parametreleri olarak değerlendirilmiştir. Son olarak, sürtünme karıştırma nokta kaynağı işleminden sonra yüzey ve hacimsel süreksizliklerin zararlı etkilerini ortadan kaldırmak için ve yapısal bütünlüğü sağlamak amacıyla çeşitli tahribatsız muayene yöntemleri önerilmiştir.

Anahtar kelimeler: Sürtünme karıştırma nokta kaynağı, Sonlu elemanlar analizi, Magnezyum alaşımı (AZ91), Eksenel kuvvet, Dönme hızı, Tahribatsız muayene

1 Introduction

Friction stir spot welding (FSSW) is a solid-state welding process and one of the innovative methods to join specifically automotive components. The conventional method was invented by Mazda Motor Cooperation in 1993 [1]. The temperatures are below the workpiece melting temperature through the tool-workpiece interface that prevents metallurgical problems via fusion process and frictional heating and plastic deformation occurs during the process. FSSW has not been tested for long term service conditions for automotive components and suffers from thermomechanical effected zones which have effects similar effects of heat affected zones (HAZ) as observed in conventional welding methods. For automotive applications solid state methods can be applicable to join vehicle body components, wheel rims, suspension arm struts for aluminium alloys (i.e. Al 2219), magnesium alloys (i.e. AZ91) and other similar and dissimilar materials (i.e. zinc and copper) to replace electric resistance spot welding [2]. The vehicle body structure components requires, on average 4000 to 6000 spot welds where these sections are critical zones for the entire structure [3]. The solid-state welding processes have some advantages towards bolted and riveted

* Sorumlu yazar / Corresponding author, e-posta / e-mail: ysarikavak@aybu.edu.tr (Y. Sarıkavak)
Geliş / Recieved: 30.08.2023 Kabul / Accepted: 11.09.2023 Yayımlanma / Published: 15.10.2023
doi: 10.28948/ngmuh.1352828

joints where improved strength, decreased costs and rigidity promotes the application of these methods [4]. Recently magnesium alloys are promising materials where combination of high strength and low density can be observed to improve vehicle performance and reduce emissions and fuel consumption in structural materials for automotive applications [5, 6]. To decrease the emissions and meet the requirements of the international environmental norms several alternative automotive applications are suggested such as shifting to hydrogen powered vehicles [7]. Thus, for the lightweight materials that contribute the decrease in emissions solid state welding is applicable for lightweight magnesium alloys. The FSSW and friction stir weld (FSW) are innovative joining processes for automotive components that are difficult to weld by conventional methods [6]. Several studies exist in literature that investigates several aspects of the FSSW in automotive applications.

Su et al. [8] investigated the formation of local melted film during FSSW of AZ91. The temperature around the rotating pin ranges 438 to 454 ºC during the process. The tool and pin diameters are 10 mm and 4 mm with rotational speed of 3000 rpm and a plunge rate of 2.5, 5 and 25 mm/s. K-type thermocouples are located 1 mm below the AZ91 material and 2 mm away from the tool pin-shoulder. Gerlich et al. [9] investigated the FSSW of similar and dissimilar aluminium (Al6111 and Al2024) and magnesium alloys (AZ91) under rotation speed of 2500 rev/min and a 4 s dwell period. K-type thermocouples located 0.8 mm from the outer periphery of the tool shoulder. The tool and pin diameters are 10 mm and 4 mm respectively. The investigated experimental peak temperatures are at the base of the pin are 531ºC, 495ºC, and 462º C for Al6111, Al2024 and AZ91 respectively. Yamamoto et al. [10] analysed the liquid penetration induced cracks during FSSW of AZ91, AZ31 and AM60. The cracking and axial pressures during FSSW of dissimilar AM60 AZ91 were investigated by Yamamoto et al. [11] where liquation cracking is a factor for joining the dissimilar AM60/AZ91 materials and cracking occurs in the thermomechanical affected zone (TMAZ). Zhang et al. [12] investigated the effect of plunge depth on microstructure and fracture in FSSW. Plunge depths of 2.0 and 2.5 mm analysed with 1400 rpm rotational speed and 0.9 m/s plunge speed.

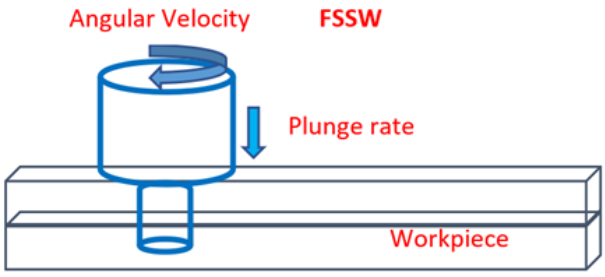

Figure 1. Schematic representation of FSSW process [13]

The finite element models (FEM) to simulate FSSW process conducted by various researchers to simulate three main steps of plunging, stirring, and retraction where experimental processes are time consuming and requires high cost. The schematic representation of FSSW can be seen in Figure 1 [13]. Constantin et al. [13] developed a FEM to join Al6061-T6 by a fully coupled thermal-stress three dimensional model and the model validated with the experimental data published in the literature. Jedrasiak et al. [14] developed a thermal model for FSSW process. Al-Al and Al-Steel automotive sheet alloys are joined in the developed model. H13 tool steel with 10 mm diameter used and K-type thermocouples installed for the process. The maximum heat input and temperature rise occurs during the dwell section in FSSW. The 2000 rpm rotational speed and 150 and 100 mm/s plunge rates are setted during the process. The convection and radiation heat transfers negleted in the study.

In recent years solid state welding processes frequently applied for many industry fields that includes automotive industry. For the resistance spot welding process automated ultrasonic inspection of weld nugget is applicable for various automotive components [15-17]. FSW and FSSW are the applicable methods for joining dissimilar and difficult to weld materials. The post weld and during the service conditions, it is important to evaluate the non-destructive testing (NDT) methods to secure structural integrity in critical components specifically after welding processes for different purposes of vehicle body components [18]. To detect and characterize discontinuities various applications exist for different targets. Main types of NDT methods are the visual inspection (optical), ultrasound inspection and advanced ultrasonic laser and phased array methods [15, 19]. Various other methods are applicable such as acoustic emission, radiography, thermography, magnetic particle inspection and liquid penetrant testing [3, 4, 20]. Various optical methods are under application and development for structural components and lifeline structures in the field [21].

Therefore, in this study magnesium alloy (AZ91) materials used for the simulation process of FSSW for the sheet metals in automotive applications. Effect of axial force, rotational speed and their effect on temperature distribution is investigated by using finite element analysis method. The analysed axial forces are ranging from 1 kN to 8 kN and 1000 rpm to 4000 rpm rotational speeds simulated to investigate heat flux and temperature rise that leads defect formation after the process. Finally, several non-destructive inspection methods are suggested to secure structural integrity after the FSSW process.

2 Materials and method

The material employed for the validation process is AZ91 sheet with 6.3 mm thick sheet where FSSW tool is made of H13 steel, shoulder and pin diameters are 10 mm and 4 mm respectively. Rotational speed during the process is 3000 rpm with 4s dwell period [8]. The maximum axial pressure during the process is 4.5 kN [9].

2.1 Numerical model

The process basically consists of various stages as initially in the tool-workpiece interface touchdown of the pin occurs and then start of pin penetration to the plunge, end of plunge and contact of shoulder in the dwell period occurs and

process finalize with the retraction of the tool [22]. Plunge, dwell and retraction are the basic three steps during the process.

The volumetric heat flux with gaussian distribution applied during the process [23]. The heat input during the process can be seen in Figure 2 [14].

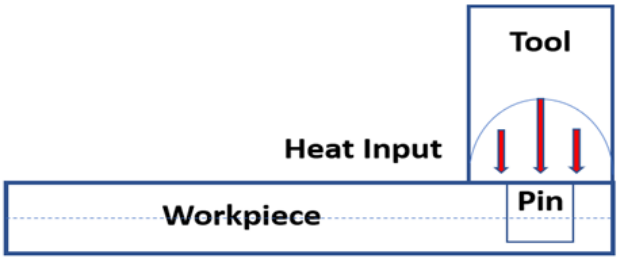

Figure 2. Schematic representation of heat input during FSSW processes via tool/pin [14]

In Equation (1) the heat flux tool/pin and workpiece interface due to friction is [22];

$$q_f = n\tau s \tag{1}$$

Where n is the fraction of frictional work converted to heat, τ is the frictional stress in 'Pa', and s is the slip rate 'm.s-1' and the frictional stress can be expressed as (Equation (2));

$$\tau = \mu(T).P(T) \tag{2}$$

Where μ is the friction coefficient, P is the contact pressure in 'Pa' and T is the temperature. In Equation (3) the frictional heat dependent to tool dimensions, rotational speed and axial force can be expressed as [24, 25];

$$q_f = 2\pi\mu RNF_n \tag{3}$$

Where R is the tool radius, N is the rotational speed of the tool/pin and F_n is the axial force. Equation (4) shows the heat flux due to conduction [22];

$$q_c = \mathrm{k(h,P,T)}(T_1 - T_2) \tag{4}$$

Where h is the overclosure (penetration of master surface) in 'm' and the P is the contact pressure [22]. The three-dimensional heat conduction equation in the workpiece is (Equation (5)) [25, 26];

$$\rho c\left(\frac{\partial T}{\partial t}\right) = \frac{\partial}{\partial x}\left(k_x\frac{\partial T}{\partial x}\right) + \frac{\partial}{\partial y}\left(k_y\frac{\partial T}{\partial y}\right) + \frac{\partial}{\partial z}\left(k_z\frac{\partial T}{\partial z}\right) + q \tag{5}$$

Where T is the time dependent temperature, c is the specific heat, ρ is the density, k_x, k_y, k_z are the heat conductivities in three perpendicular directions and q is the generated heat during the process.

To simulate workpiece material behaviour for elastic plastic model, strain rate and temperature dependent Johnson-Cook material model best fits with FSSW process as seen in Equation (6) [13].

$$\bar{\sigma} = [A + B.(\bar{\varepsilon}^{pl})^n].\left[1 + C.\ln\left(\frac{\dot{\bar{\varepsilon}}^{pl}}{\dot{\bar{\varepsilon}}_0^{pl}}\right)\right].[1 - (\frac{T - T_{ref}}{T_{melt} - T_{ref}})^m] \tag{6}$$

Where $\bar{\sigma}$ is the flow stress, $\bar{\varepsilon}^{pl}$ is the equivalent plastic strain, $\dot{\bar{\varepsilon}}^{pl}$ is the equivalent plastic strain rate, $\frac{\dot{\bar{\varepsilon}}^{pl}}{\dot{\bar{\varepsilon}}_0^{pl}}$ is the normalized equivalent plastic strain rate, A, B, C, n and m are the material constants and the exponent n considers the hardening of the material where m is dependent to melting and T_{ref} is the ambient temperature.

The density of AZ91 is 1.81 g/cm^3, thermal conductivity, specific heat and the melting temperature is 84 W/mK, 1 J/g ºC and ≥421 ºC respectively. The tensile yield strength, and tensile strength is 95 MPa and 125 MPa, respectively. At the top surface of the workpiece convective heat transfer coefficient defined as h=30 W/m^2-ºC. Conduction heat transfer defined for the workpieces and at the bottom of the workpiece with a value of 100000 W/m^2-ºC [13].

During the FSSW process axial pressure ranges up to 14 kN under 3000 rpm rotational speed [11]. The midway of the dwell period the highest axial pressures can be observed and it gradually decreases with time until the end of the FSSW process. Thus, various axial pressures of the tool-pin material analysed considering the values of 1 kN, 2 kN, 3 kN, 4.5 kN, 8 kN for the simulation process, respectively.

3 Results and discussion

3.1 Validation

The K-type thermocouple was installed 1 mm below the upper surface of the sheet around the pin periphery (0.4 mm apart) with a tool rotational speed of 3000 rpm, 4.5 kN axial force, a plunge rate of 2.5 mm/s with 4 s dwell period [8]. The temperature distribution with the FEM through the thickness can be seen in Figure 3. The obtained FEM result 1 mm below the upper surface around the pin periphery is 453.8 ºC as seen in Figure 3.

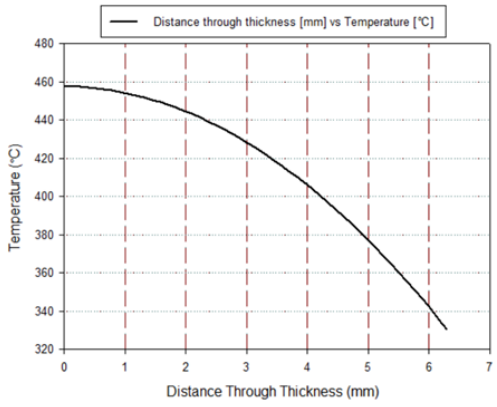

Figure 3. FEM results of temperature distribution through thickness under experimental conditions

The experimental result measured via K-type thermocouple is 453 ºC as the maximum value at the same location [8]. This maximum temperature decreases to 438 ºC through the dwell period during FSSW with time. As seen here experimental and the FEM results are almost same and the developed model gives consistent results for the FSSW process.

3.2 *Effect of axial pressure in FSSW*

The developed FEM employed under various boundary conditions. One of the major parameters for an effective weld without defect formation is the applied axial force. It is clearly observed that the peak temperature during the process shows significant change under different axial force during the process (see Figure 4). For the experimental value of 4.5 kN axial force, the analysed maximum temperature under the sheet surface is 457.6 ºC and this value decreases through the thickness. This temperature decreases and increases according to the change in axial force as well. The 1 kN axial force resulted with 116.4 ºC at the top of the sheet material which this thermal change will not lead softening of the sheet metal sufficiently and will not lead any microstructural change during the process.

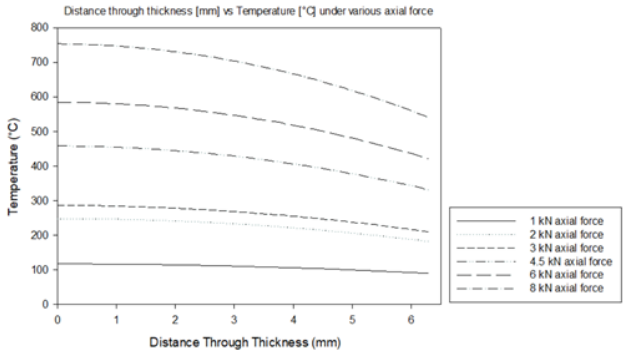

Figure 4. Temperature distribution under various axial force in FSSW

Increase in axial force resulted with increase in the peak temperature where 2 kN, 3 kN, 6 kN and 8 kN axial forces are employed for the simulation process. The obtained peak temperatures are 246.9 ºC, 285.6 ºC, 584.4 ºC, and 753 ºC respectively. The melting temperature of AZ91 is ≥421 ºC and according to these peak temperatures on pin periphery are below the melting temperature for the axial forces of 1 kN, 2 kN, 3 kN values. For the rest of the employed parameters such as 4.5 kN, 6 kN and 8 kN during the dwell period peak temperature reach above the melting temperature. The sufficient temperature to melt the workpiece result with the smooth spot weld process where insufficient temperature to soften the material may lead tool-pin consumption, failure and instable process that may lead discontinuities in the sheet metal.

In general, it is assumed that FSSW generates improved and defect free joints compared to the other welding methods (fusion welding etc.) however various defects are reported during the process according to the liquation cracking in the thermomechanically (TMAZ) affected zones. In literature [27, 28], early in the dwell period eutectic film formation and cracking observed due to the rapid dissolution of melted eutectic films. The cracking in the grain boundary regions of stir zones are reported for elevated temperatures [28]. The local melting can be observed in TMAZ for the increased axial forces that lead elevated temperatures over melting point and this results with the cracking in the sheet metal.

The operational conditions are also critical where repeated loading to the FSSWed alloy sheets may lead failure under fatigue loading conditions. Several studies reported where crack may initiate and propagate at the tongue like region in the weld area. Luo et al. [29] reported that primary stage of crack propagation exist in the outer section of the weld area and propagates along the interface of heat affected zone (HAZ) and TMAZ across the direction of the force. Thus, internal cracks in the HAZ and TMAZ sections [29] and lack of mixing, incomplete refill, contamination and combination of these defects [30] are possible defect types that can be considered in terms of lifetime monitoring and quality check in terms of non-destructive inspection perspective.

3.3 *Effect of rotational speed in FSSW*

The other important process parameter for FSSW is the rotational speed of the tool/pin material.

The tool material of H13 steel used for the process and effect of rotational speed for heat flux and temperature rise investigated for the values ranging from 1000 rpm to 4000 rpm. Figure 5 shows the effect of rotational speed on temperature through the thickness of the sheet. The investigated maximum temperature for 1000 rpm rotational speed is 171.6 ºC and this gradually decreases through the thickness to 128.1 ºC at the bottom of the sheet material. For 2000 rpm at the top and bottom of the sheet 298.2 ºC and 217.9 ºC investigated, respectively. The 3000 rpm and 4000 rpm rotational speeds results with 457.6 ºC; 330.5 ºC and 550.9 ºC; 397.3 ºC at the top and bottom surface of the sheet. Thus, according to the simulated results 3000 rpm and 4000 rpm boundary conditions results with the temperatures over the melting point of the AZ91.

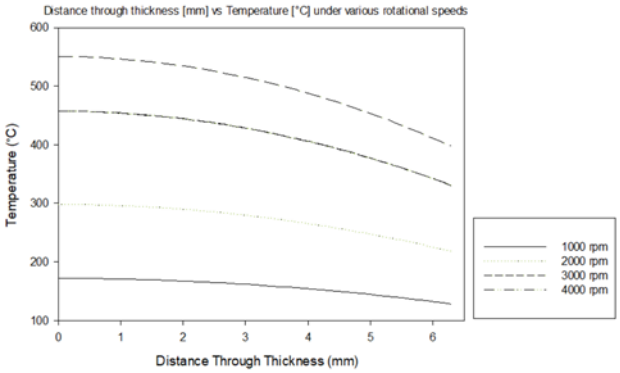

Figure 5. Effect of rotational speed on temperature in FSSW

3.4 *Non-Destructive Inspection (NDI) approach for FSSWed joints*

Considering the process temperatures and heat flux occurred during the operation in FSSW both internal and

surface cracks (thermal) can be observed. For the volumetric defects acoustic emission and various types of ultrasonic inspection methods are candidate methods for structural integrity in the FSSWed automotive and vehicle components. Real time monitoring during the process, post weld inspection and detection under service conditions for specified time periods are critical based on the application area, process parameters and employed materials. Dahmane et al. [30] employed real time acoustic emission for detection of discontinuities and on the other hand, Zhang et al. [31] used the non-contact laser ultrasonic inspection for discontinuity detection in FSSW process. Non-contact methods are relatively easy to apply and results with feasible applications under field conditions such as in service applications [32]. The contact ultrasonic pulse echo method is relatively less in cost and feasible for inspection after manufacture. Considering the thickness of the sheet alloys inspection frequency in ultrasonic method should be well arranged to obtain accurate results.

The thermal cracks and other surface defects dependent to process parameters are possible surface discontinuities in FSSW. For the defect and discontinuity detection which are located on the surface of the workpiece, initially visual inspection is an important method prior to the other inspection methods. The liquid penetrant and magnetic particle inspection methods are other applicable methods for surface defects after FSSW. Thus, for volumetric and surface defect combinations one of the volumetric methods of ultrasonic or acoustic emission tests can be applicable where for the surface detection visual inspection and magnetic particle or liquid penetrant tests are other possible candidate methods for structural integrity.

4 Conclusions

In this study finite element-based process simulation of FSSW conducted. Various aspects considered during the simulation and effect of axial force and rotational speed in terms of temperature rise evaluated in detail for various levels range between 1 kN to 8 kN and 1000 rpm to 4000 rpm. Temperature rise that leads crack formation during the process evaluated and considering possible discontinuity types several non-destructive inspection methods are suggested for FSSW process under real time monitoring, after manufacturing and under service conditions for automotive applications. Below conclusions can be drawn:

Increase in axial force resulted with increase in the peak temperatures. The various axial force is employed ranging from 1 kN to 8 kN for the simulation process. The obtained peak temperatures are 116.4 ºC, 246.9 ºC, 285.6 ºC, 457.6 ºC, 584.4 ºC, and 753 ºC respectively for 1 kN, 2 kN, 3 kN, 4.5 kN, 6 kN and 8 kN axial forces.

For 3000 rpm rotational speed, temperatures are over melting point for 4.5 kN, 6 kN and 8 kN axial forces, thus these forces are the critical values in terms of defect and crack formation during the process under specified conditions.

The results under 4.5 kN axial force and 3000 rpm to 4000 rpm shows increased temperatures that are over the melting point of AZ91.

The developed model for the simulation of FSSW is validated considering the experimental results reported in the literature thus, other process parameters can be simulated to evaluate peak temperature, the temperature distribution and defect formation for the process.

For the volumetric discontinuities ultrasonic and acoustic inspection and for the surface defects visual, magnetic particle or liquid penetrant test methods are effective methods for structural integrity considering the possible discontinuities dependent to process physical nature.

Conflict of interest

The author declares that there is no conflict of interest.

Similarity rate (iThenticate): 19%

References

[1] X. W. Yang, T. Fu and W. Y. Li, Friction stir spot welding: a review on joint macro and microstructure, property, and process modelling. Advances in Materials Science and Engineering, 697170, 1–11, 2014. https://doi.org/10.1155/2014/697170.

[2] M. A. Omar, The Automotive Body Manufacturing Systems and Processes. John Wiley & Sons Ltd., Chichester, UK, 2011.

[3] J. Chen and Z. Feng, IR-based spot weld NDT in automotive applications. Proceedings, Thermosense: Thermal Infrared Applications XXXVII; 9485, Baltimore, United States, 2015. https://doi.org/10.1117/12.2177124.

[4] M. M. Shtrikman, Current state and development of friction stir welding Part 3. Industrial application of friction stir welding. Welding International, 22, 806–815, 2008. https://doi.org/10.1080/09507110802593620.

[5] O. Torun and I. Celikyurek, The effect of the friction pressure on the friction welding of AZ91 and Fe_3Al alloys. The Eurasia Proceedings of Science, Technology, Engineering & Mathematics, 7, 175–180, 2019.

[6] C. Blawert, N. Hort and K. U. Kainer, Automotive applications of magnesium and its alloys. Transactions of The Indian Institute of Metals, 57, 397–408, 2004.

[7] M. Ciniviz and H. Köse, Hydrogen use in internal combustion engine: a review. International Journal of Automotive Engineering and Technologies, 1, 1–15, 2012.

[8] P. Su, A. Gerlich, M. Yamamoto and T. H. North, Formation and retention of local melted films in AZ91 friction stir spot welds. Journal of Materials Science, 42, 9954–9965, 2007. https://doi.org/10.1007/s10853-007-2061-4.

[9] A. Gerlich, P. Su and T. H. North, Peak temperatures and microstructures in aluminium and magnesium alloy friction stir spot welds. Science Technology of Welding and Joining, 10, 647–652, 2005. https://doi.org/10.1179/174329305X48383.

[10] M. Yamamoto, A. Gerlich, T. H. North and K. Shinozaki, Liquid penetration induced cracking in Mg-alloy spot welds. Materials Science Forum, 580–582,

409–412, 2008. https://doi.org/10.4028/www.scientific.net/msf.580-582.409.
[11] M. Yamamoto, A. Gerlich, T. H. North and K. Shinozaki, Cracking in dissimilar Mg alloy friction stir spot welds. Science and Technology of Welding and Joining, 13, 583–592, 2008. https://doi.org/10.1179/174329308X349520.
[12] H. F. Zhang, L. Zhou and W. Li, Effect of tool plunge depth on the microstructure and fracture behavior of refill friction stir spot welded AZ91 magnesium alloy joints. International Journal of Minerals, Metallurgy and Materials, 28, 699–709, 2021. https://doi.org/10.1007/s12613-020-2044-x.
[13] M. A. Constantin, A. Boşneag, M. Iordache, C. Bădulescu and E. Niţu, Numerical simulation of friction stir spot welding. Applied Mechanics and Materials, 834, 43–48, 2016. https://doi.org/10.4028/www.scientific.net/AMM.834.43.
[14] P. Jedrasiak, H. R. Shercliff and A. Reilly, Thermal modeling of Al-Al and Al-Steel friction stir spot welding. Journal of Materials Engineering and Performance, 25, 9, 4089–4098, 2016. https://doi.org/10.1007/s11665-016-2225-y.
[15] C. Ji, J. K. Na, Y. S. Lee, Y. Do Park and M. Kimchi, Robot-assisted non-destructive testing of automotive resistance spot welds. Welding in the World, 73, 6, 753–763. 2021. https://doi.org/10.1007/s40194-020-01002-1.
[16] P. Buschke, W. Roye and T. Dahmen, Multiple NDT methods in the automotive industry. Huerth, Germany, 2002.
[17] S. A. Titov, R. G. Maev and A. N. Bogachenkov, Pulse-echo NDT of adhesively bonded joints in automotive assemblies, Ultrasonics, 48, 6–7, 537–546, 2008. https://doi.org/10.1016/j.ultras.2008.07.001.
[18] Z. Wu, X. Zhou, N. Ao, X. Han, Z. Zhu and S. Wu, Tensile and fatigue behaviors of hybrid laser welded A7N01 alloy with repairing for railway vehicles. Engineering Failure Analysis, 143, 1–15, 2023. https://doi.org/10.1016/j.engfailanal.2022.106930.
[19] M. Thornton, L. Han and M. Shergold, Progress in NDT of resistance spot welding of aluminium using ultrasonic C-scan. NDT&E International, 48, 30–38, 2012. https://doi.org/10.1016/j.ndteint.2012.02.005.
[20] H. Taheri, M. Kilpatrick, M. Norvalls, W. J. Harper, L. W. Koester, T. Bigelow and L. J. Bond, Investigation of nondestructive testing methods for friction stirwelding. Metals (Basel), 9, 6, 1–22, 2019. https://doi.org/10.3390/met9060624.
[21] Y. K. Zhu, G. Y. Tian, R. S. Lu and H. Zhang, A review of optical NDT technologies. Sensors, 11, 8, 7773–7798, 2011. https://doi.org/10.3390/s110807773.
[22] S. U. Khosa, T. Weinberger and N. Enzinger, Thermo-mechanical investigations during friction stir spot welding (FSSW) of AA6082-T6. Welding in the World, 54, 134–146, 2010. https://doi.org/10.1007/BF03263499.
[23] P. Jedrasiak and H. R. Shercliff, Small strain finite element modelling of friction stir spot welding of Al and Mg alloys. Journal of Materials Processing Technology, 263, 18, 207–222, 2019. https://doi.org/10.1016/j.jmatprotec.2018.07.031.
[24] M. Awang, V. H. Mucino, Z. Feng and S. A. David, Thermo-mechanical modeling of friction stir spot welding (FSSW). SAE International, 724, 2006. https://doi.org/10.4271/2006-01-1392.
[25] M. Awang, Simulation of friction stir spot welding (FSSW) process : study of friction phenomena, West Virginia University, USA, 2007.
[26] Y. Sarikavak, An advanced modelling to improve the prediction of thermal distribution in friction stir welding (FSW) for difficult to weld materials. Journal of Brazilian Society of Mechanical Sciences and Engineering, 43, 4, 1-14 2021. https://doi.org/10.1007/s40430-020-02735-2.
[27] M. Yamamoto, A. Gerlich, T. H. North and K. Shinozaki, Mechanism of cracking in AZ91 friction stir spot welds. Science and Technology of Welding and Joining, 12, 3, 208–216, 2007. https://doi.org/10.1179/174329307X177900.
[28] M. Yamamoto, A. Gerlich, T. H. North and K. Shinozaki, Cracking in the stir zones of Mg-alloy friction stir spot welds, Journal of Materials Science, 42, 18, 7657–7666, 2007. https://doi.org/10.1007/s10853-007-1662-2.
[29] T. J. Luo, B. L. Shi, Q. Q. Duan, J. W. Fu and Y. S. Yang, Fatigue behavior of friction stir spot welded AZ31 Mg alloy sheet joints. Transactions of Nonferrous Metals Society of China, 23, 7, 1949–1956, 2013. https://doi.org/10.1016/S1003-6326(13)62682-5.
[30] F. Dahmene, S. Yaacoubi, M. E. Mountassir, G. Porot, M. Masmoudi, P. Nennig, U. F. H. Suhuddin and J. F. Santos, Dataset from healthy and defective spot welds in refill friction stir spot welding using acoustic emission. Data in Brief, 45, 108750, 2022. https://doi.org/10.1016/j.dib.2022.108750.
[31] K. Zhang, Z. Zhou and J. Zhou, Application of laser ultrasonic method for on-line monitoring of friction stir spot welding process, Applied Optics, 54, 25, 7483, 2015. https://doi.org/10.1364/ao.54.007483.
[32] Z. Zhou and K. Zhang, Evaluation of friction stir spot welding process by laser ultrasonic method with synthetic aperture focusing technique. 19th World Conference on Non-Destructive Testing, Munich, Germany, 13-17 June 2016.